

Instruments and Methods

A scanning electron microscope technique for identifying the mineralogy of dust in ice cores

Rachel W. OBBARD,¹ Ian BAKER,¹ David J. PRIOR²

¹*Thayer School of Engineering, Dartmouth College, Hanover, New Hampshire 03755-8000, USA*
E-mail: Rachel.W.Obbard@dartmouth.edu

²*Department of Earth and Ocean Sciences, Liverpool University, 4 Brownlow Street, Liverpool L69 3GP, UK*

ABSTRACT. Dust particles in an ice core from East Rongbuk Glacier on the northern slope of Qomolangma (Mount Everest; 28°01' N, 86°58' E; 6518 m a.s.l.), central Himalaya, have been identified as mica using a combination of scanning electron microscope-based techniques and energy-dispersive X-ray spectroscopy to identify the elements present, and electron backscatter diffraction to identify the crystal type. This technique for identifying individual crystalline dust particles in samples of glacial ice could be especially useful in the future for identifying water-soluble crystals in ice, for studying the strain history (glaciotectionics) of basal ice or in studies of ice–mica composites used as analogs of quartz-mica rocks.

INTRODUCTION

Glaciers are natural archives of atmospheric change. Ice-core records from high-elevation remote locations in the central Himalayan region have been compared with those from the polar regions to better understand atmospheric circulation patterns and climate change (Yao and others, 2002; Thompson and others, 2006). The meteorological regime of the Asian continent is controlled by air masses from the continent itself, as well as from the Arctic and the Pacific and Indian Oceans (Bryson, 1986). High on a northwest ridge of Qomolangma (Mount Everest) the 48 km² East Rongbuk Glacier lies near the continental divide and is exposed to both the continental air masses of central Asia, westerlies in the winter months and the Indian monsoon in the summer (Kang and others, 2004; Xu and others, 2009b, 2010). An excellent figure showing the location, distribution of dust sources and general winter and summer circulation patterns is included in Xu and others (2009b, 2010). These authors found that dust (insoluble particle) concentration at the location is highest during warm dry periods and lower during cold humid periods such as the Little Ice Age, despite increased winds during the latter (Xu and others, 2010). Dust from the arid Tibetan Plateau contributes Ca²⁺ and Mg²⁺ to the ice, while Na⁺ and Cl⁻ come from a strong marine contribution during the summer monsoon season (Kang and others, 2000) as well as from evaporite deposits on the Tibetan Plateau (Wake and others, 2001). SO₄²⁻ and NO₃⁻ can arise from continental dust, biomass burning and local acidic gases (Kang and others, 2000). East Rongbuk Glacier has a high ammonium background due to the proximity of local sources (NH₄⁺ is related to agricultural production; Hou and others, 2003) and to biomass burning and other natural as well as human causes.

An 80.4 m core obtained from the glacier in 1998 was dated by noting the seasonal variations of stable-isotopic and major-ionic profiles and comparing the result with double β activity horizons from atmospheric thermonuclear tests conducted in the 1950s and 1960s (Hou and others, 2003). Sulfate peaks from a series of volcanic events in Japan

and Indonesia and a sodium peak from a monsoon were also used as dating horizons (Hou and others, 2003).

In 2002, University of Maine (Orono, USA) Climate Change Institute scientists and their Chinese colleagues drilled East Rongbuk Glacier to bedrock and collected a 108.83 m ice core. This was dated to 98 m (AD 1534 \pm 5) by counting the seasonal variations of the stable-isotopic and major-ionic profiles (e.g. CH₄ and $\delta^{18}\text{O}_{\text{atm}}$). The portion below 98 m was dated using a flow model that constrained the age of the deepest 2 m using CH₄ and $\delta^{18}\text{O}_{\text{atm}}$ values, resulting in a maximum age of 1498–2055 BP (Hou and others, 2004; Xu and others, 2009a).

We received samples of ice from the lower part of the core and describe herein a method of identifying the mineralogy of crystalline dust particulates in ice samples using the combination of two characterization techniques.

MATERIALS AND METHODS

The 9 cm diameter East Rongbuk core was analyzed using the continuous melting with discrete sampling (CMDS) system at the Climate Change Institute (Osterberg and others, 2006). This technique melts a square section 4 cm on a side from the center of the core, leaving slabs from the outside of the core. Five of these remnants, each approximately 6–12 cm long and 1–2 cm thick, were sent to Dartmouth College. They came from 1 m core sections between 88 and 107 m, but exact sample depths are uncertain because the remnants had not been labeled when separated from the core (they were not intended for later use). Therefore, depth uncertainty may be almost as much as 1 m and comparisons of impurities in our samples with core chemistry measured with the CMDS system cannot be made.

The samples were stored at -25°C to -35°C and held below -10°C during overnight transfer to Dartmouth. We used an FEI XL-30 environmental scanning electron microscope (SEM) with a liquid-nitrogen-chilled cold stage. Our technique for sample preparation and scanning

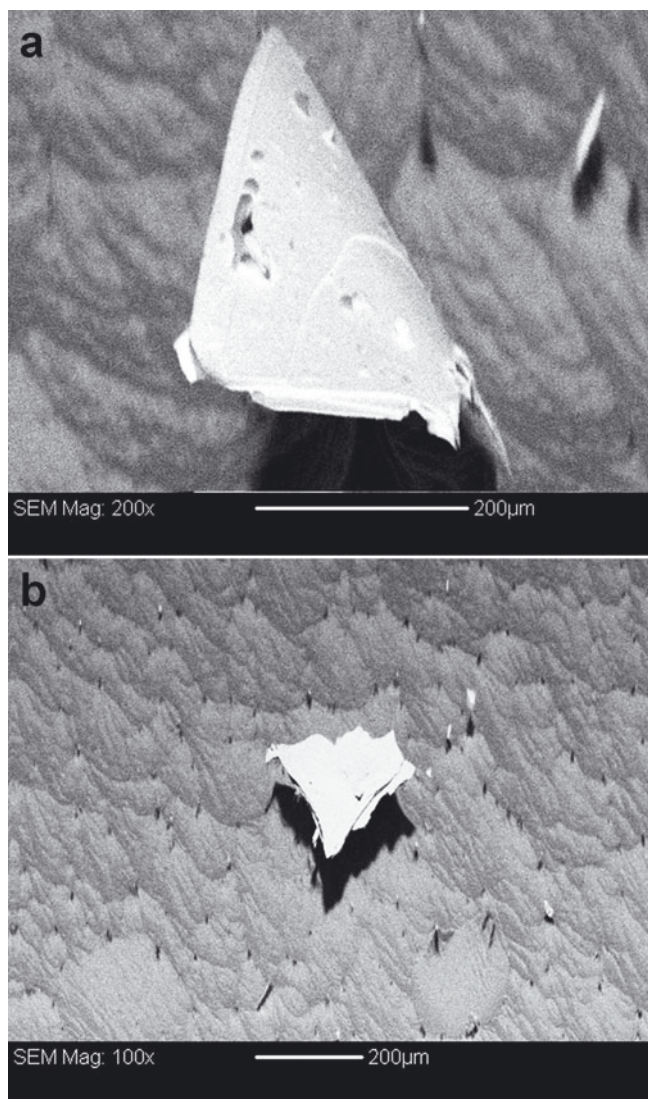


Fig. 1. Secondary electron images of 200 µm dust particles found at 107 m.

electron microscopy and energy-dispersive spectroscopy (EDS) of uncoated ice in the FEI XL-30 SEM is described in detail by Iliescu and others (2004). We worked under a High Efficiency Particle Air (HEPA)-filtered laminar-flow hood and handled samples with polyethylene gloves and tools cleaned thoroughly with a regimen of acetone, methanol, *n*-hexane and deionized water. First, the outside 1–2 mm of the samples (which could have been contaminated by handling) were removed. Then samples of ice 10 mm × 5 mm × 3 mm were cut perpendicular to the sides of the core, smoothed with a razor blade and placed in a pre-cleaned sealed container at -25°C for 24 hours so that sublimation would cause further smoothing of the surface. Once in the SEM, the samples were held at $-85 \pm 5^{\circ}\text{C}$, a temperature chosen because it allows sufficient sublimation to prevent charge build-up on the surface of the sample. Our electron backscatter diffraction (EBSD) technique is described in detail by Iliescu and others (2004) and Obbard and others (2006).

In this paper, we describe the identification of the mineralogy of dust particles in the core using a combination of EDS and EBSD.

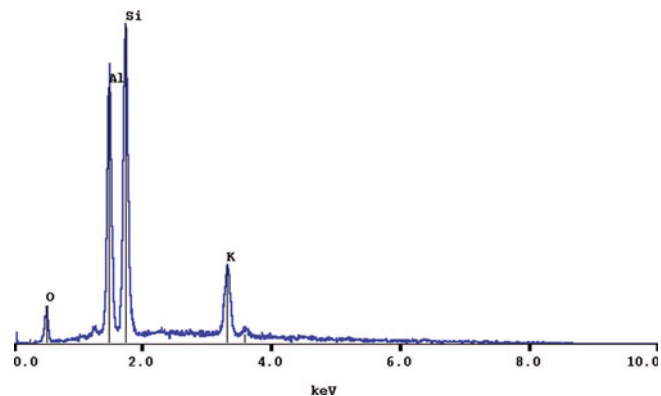


Fig. 2. EDS spectrum (1475 counts full scale) from the large dust particle found at 107 m shown in Figure 1a.

RESULTS

The sample from 107.07 to 107.64 m contained nine large ($>60\ \mu\text{m}$) particles within the ice crystals that were revealed during sublimation. Examples are shown in Figure 1.

Using EDS, Si, Al and K were identified in most of these particles, and Mg, Ti and Fe in some. A sample spectrum from the particle in Figure 1a is shown in Figure 2.

Diffraction patterns from the particles shown in Figure 1a and b are shown in Figure 3a and b, respectively. HKL Technology's CHANNEL 5TM software was used to index each pattern using the American Mineralogist Phase Database. The phase database contains crystallographic, compositional and diffraction pattern information for 1453 mineralogical phases, based on data from the Mineralogical Society of America's Crystal Structure Database. By narrowing our search to minerals containing the elements we found using EDS, which produced patterns matching those collected using EBSD, we identified the particles shown in Figure 1a and b (as well as four other particles found in this sample) as micas, or illite clays with high crystallinity. EBSD alone cannot distinguish different micas (or illite) and these patterns can be indexed equally well with either monoclinic muscovite or biotite structures (for example). Given that the EDS spectra indicate primarily Si, Al and K, then muscovite mica is the most likely candidate. If the Mg, Ti and Fe peaks were stronger, then biotite mica would be a better candidate. Biotite–muscovite interlayered grains are common and would have spectra that combine elements of both.

Upper-hemisphere pole figures (stereonets) for the particles analyzed and the ice crystals in this sample are shown in Figure 4. Both pole figures are oriented the same with respect to the sample, and in both the coring direction is vertical.

DISCUSSION

Mineral dust can be transported long distances by wind and, because most of the common elements (Al, Ca, Fe, K, Mg and Si) are widely distributed, its source area is generally determined more by wind patterns rather than by the elements present (Arimoto, 2001). Aeolian dust in Himalayan ice cores results primarily from westerly winds in winter, dust storms from the southern Tibetan Plateau, India and the Near East in the spring, and the south Asian monsoon in the summer (Thompson and others, 2000; Kang and others, 2002). The majority of aeolian particles are

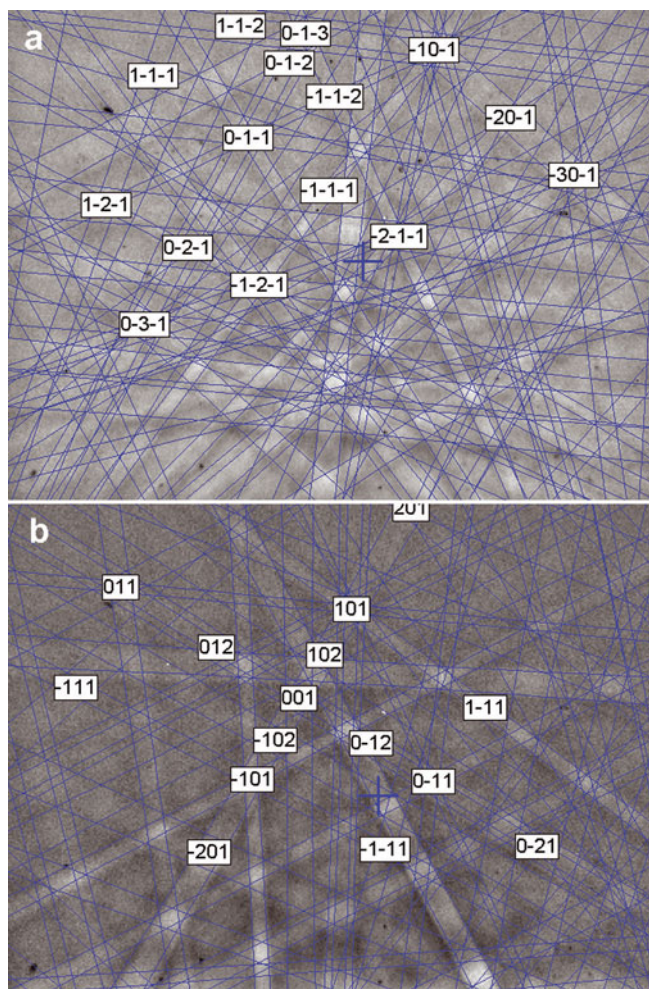


Fig. 3. EBSD patterns from impurities found at 107 m, both tentatively identified as muscovite, $KAl_2(AlSi_3O_{10})(F,OH)_2$, monoclinic. Diffraction patterns shown in (a) and (b) are from particles shown in Figure 1a and b, respectively.

fine-grained ($<63 \mu\text{m}$) clay and silt; larger-grained ($>63 \mu\text{m}$) particles are in the minority (e.g. Jiang and Ding, 2010). However, particles as large as $350 \mu\text{m}$ have been found (Jiang and Ding, 2010).

In our experience, soluble impurities containing Cl, K, Mg and S are most often $<10 \mu\text{m}$ in size and found in grain boundaries (Cullen and Baker, 2000, 2001; Baker and others, 2003; Obbard, 2006). The particles found in our East Rongbuk samples were located in the lattice (rather than in the grain boundaries), were typically $60\text{--}200 \mu\text{m}$ in size and all contained Si and Al, with some combination of K, Mg and Fe and sometimes Na, Ca and Cl. This, together with their EBSD patterns, suggests that they are micas ($(K,Na,Ca)_2(Al,Mg,Fe)_{4-6}(Si,Al)_8O_{20}(OH,F)_4$), minerals which are prevalent in the Earth's crust. Although the Al is a bit high relative to Si, the topography of the particle means that the geometries are not ideal, and relative peak height differences might be expected.

The sample from 107 m was within 2 m of the bedrock, so we did consider that these particles might be material picked up from the bedrock by the basal ice during glacier movement. In our EBSD analysis of this core (the ice), we observed single maxima in samples from 88 and 107 m (e.g. Fig. 4) and multiple maxima at 100, 104, 105 and 106 m. A single-maximum fabric suggests either uniaxial compression

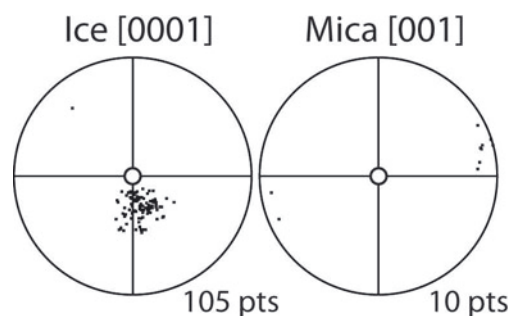


Fig. 4. Equal-area upper-hemisphere stereonet showing ice and mica *c*-axis data from the sample analyzed. The core axis is in the center of the stereonet.

or simple shear. Simple shear is caused by glaciers moving over local variations in topography and by substratum debris but occurs well above the substratum in most cases (Thorsteinsson and others, 1997). The drilling team, using GPS surveys in 1998 and 2002, found no horizontal movement at the drilling site (Xu and others, 2010). Nonetheless, the single-maximum fabric at 107 m could indicate basal shear (Kamb, 1959; Jonsson, 1970; Hambrey, 1979). This does not necessarily mean that particles found in it are from the bedrock. Since this 6 cm vertical sample contained no other signs of visible debris (Obbard, 2006), we consider it likely that these impurities are of aeolian origin.

In the EBSD patterns shown in Figure 3 (and in the patterns from the other four particles they were collected from), the basal planes are steep, i.e. the *c*-axis lies in a sub-horizontal orientation. This is in sharp contrast to the almost vertical orientation of the ice *c*-axes. Micas are platy and the plates tend to align perpendicular to shortening. If mica particles such as these are representative, then in aggregate they may contain information about the deformation kinematics and history of the ice (glaciations induced deformation in sediment). With a sufficient number of particles to assess fabric, our technique could be useful in studies of deformation of actual basal ice samples (containing more particles).

The use of this technique to orient grains in an ice–mica mixture is also interesting because such mixtures have been used in the past to simulate deformation in foliated quartz–mica rocks (Wilson, 1983, 1984). Mica is commonly foliated (layered) or found in layers separated by rock containing significant quartz. When a composite contains phyllosilicates (e.g. muscovite mica) and a more ductile phase, the phyllosilicates tend to rotate to accommodate the stress (Wilson, 1983; Dempsey and others, in press). Thus an ice–mica aggregate might be used to study deformation in mica-bearing rocks.

CONCLUSIONS

Using information obtained from both EDS and EBSD, we have identified specific particles in an ice-core sample from 107 m in East Rongbuk Glacier as micas, probably muscovite. We have also demonstrated that it is possible to identify the mineral composition of individual crystalline particles in ice cores while they are in the ice (provided they are on an exposed surface or can be exposed through sublimation). In this respect, the technique has advantages over X-ray diffraction in that single particles can be

examined and need not be removed from the ice (important in the case of water-soluble particles). Moreover, this technique may also be useful for studying the strain history (glaciotectonics) of basal ice or in studies of ice–mica composites used as analogs of the quartz–mica system.

ACKNOWLEDGEMENTS

This research was supported by the US National Science Foundation grants OPP-0221120. We thank the University of Maine Climate Change Institute for providing the specimens for this study, and two anonymous reviewers whose thoughtful comments added much to the paper.

REFERENCES

- Arimoto, R. 2001. Eolian dust and climate: relationships to sources, tropospheric chemistry, transport and deposition. *Earth-Sci. Rev.*, **54**(1–3), 29–42.
- Baker, I., D. Cullen and D. Iliescu. 2003. The microstructural location of impurities in ice. *Can. J. Phys.*, **81**(1–2), 1–9.
- Bryson, R.A. 1986. Airstream climatology of Asia. In *Proceedings of the International Symposium on the Qinghai–Xizang Plateau and Mountain Meteorology, 20–24 March 1984, Beijing, China*. Boston, MA, American Meteorological Society, 604–617.
- Cullen, D. and I. Baker. 2000. Correspondence. The chemistry of grain boundaries in Greenland ice. *J. Glaciol.*, **46**(155), 703–706.
- Cullen, D. and I. Baker. 2001. Observation of impurities in ice. *Microsc. Res. Technol.*, **55**(3), 198–207.
- Dempsey, E., D. Prior, E. Mariani, V. Troy and D.J. Tatham. In press. Mica controlled anisotropy within mid to upper crustal mylonites: an EBSD study of mica fabrics in the Alpine Fault Zone, New Zealand. In Prior, D., E.H. Rutter and D.J. Tatham, eds. *Deformation mechanisms, rheology and tectonics: current status and future perspectives*. London, Geological Society of London.
- Hambrey, M.J. 1979. Crystal orientation fabrics in relation to structures and strain, Griesgletscher, Valais, Switzerland. *Z. Gletscherkd. Glazialgeol.*, **15**(1), 73–86.
- Hou, S., D. Qin, D. Zhang, S. Kang, P.A. Mayewski and C.P. Wake. 2003. A 154 a high-resolution ammonium record from the Rongbuk Glacier, north slope of Mt. Qomolangma (Everest), Tibet–Himal region. *Atmos. Environ.*, **37**(5), 721–729.
- Hou, S. and 7 others. 2004. Correspondence. Age of Himalayan bottom ice cores. *J. Glaciol.*, **50**(170), 467–468.
- Iliescu, D., I. Baker and H. Chang. 2004. Determining the orientations of ice crystals using electron backscatter patterns. *Microsc. Res. Technol.*, **63**(4), 183–187.
- Jiang, H. and Z. Ding. 2010. Eolian grain-size signature of the Sikouzi lacustrine sediments (Chinese Loess Plateau): implications for Neogene evolution of the East Asian winter monsoon. *Geol. Soc. Am. Bull.*, **122**(5–6), 843–854.
- Jonsson, S. 1970. Structural studies of subpolar glacier ice. *Geogr. Ann.*, **52A**(2), 129–145.
- Kamb, W.B. 1959. Ice petrofabric observations from Blue Glacier, Washington, in relation to theory and experiment. *J. Geophys. Res.*, **64**(11), 1891–1909.
- Kang, S., C.P. Wake, D. Qin, P.A. Mayewski and T. Yao. 2000. Monsoon and dust signals recorded in Dasuopu Glacier, Tibetan Plateau. *J. Glaciol.*, **46**(153), 222–226.
- Kang, S. and 7 others. 2002. Glaciochemical records from a Mt. Everest ice core: relationship to atmospheric circulation over Asia. *Atmos. Environ.*, **36**(21), 3351–3361.
- Kang, S.C., P.A. Mayewski, D.H. Qin, S.A. Sneed, J.W. Ren and D.Q. Zhang. 2004. Seasonal differences in snow chemistry from the vicinity of Mt. Everest, central Himalayas. *Atmos. Environ.*, **38**(18), 2819–2829.
- Obbard, R. 2006. Microstructural determinants in glacial ice. (PhD thesis, Dartmouth College.)
- Obbard, R., I. Baker and K. Sieg. 2006. Using electron backscatter diffraction patterns to examine recrystallization in polar ice sheets. *J. Glaciol.*, **52**(179), 546–557.
- Osterberg, E.C., M.J. Handley, S.B. Sneed, P.A. Mayewski and K.J. Kreutz. 2006. Continuous ice core melter system with discrete sampling for major ion, trace element, and stable isotope analyses. *Environ. Sci. Technol.*, **40**(10), 3355–3361.
- Thompson, L.G., T. Yao, E. Mosley-Thompson, M.E. Davis, K.A. Henderson and P. Lin. 2000. A high-resolution millennial record of the south Asian monsoon from Himalayan ice cores. *Science*, **289**(5486), 1916–1919.
- Thompson, L.G. and 6 others. 2006. Ice core evidence for asynchronous glaciation on the Tibetan Plateau. *Quat. Int.*, **154/155**, 3–10.
- Thorsteinsson, T., J. Kipfstuhl and H. Miller. 1997. Textures and fabrics in the GRIP ice core. *J. Geophys. Res.*, **102**(C12), 26,583–26,599.
- Wake, C.P. and 6 others. 2001. Changes in atmospheric circulation over the South-Eastern Tibetan Plateau over the last two centuries from a Himalayan ice core. *PAGES News*, **9**(3), 14–16.
- Wilson, C.J.L. 1983. Foliation and strain development in ice–mica models. *Tectonophysics*, **92**(1–3), 93–122.
- Wilson, C.J.L. 1984. Shear bands, crenulations and differential layering in ice–mica models. *J. Struct. Geol.*, **6**(3), 303–319.
- Xu, J. and 6 others. 2009a. Records of volcanic events since AD 1800 in the East Rongbuk ice core from Mt. Qomolangma. *Chinese Sci. Bull.*, **54**(8), 1411–1416.
- Xu, J., S. Hou, F. Chen, J. Ren and D. Qin. 2009b. Tracing the sources of particles in the East Rongbuk ice core from Mt. Qomolangma. *Chinese Sci. Bull.*, **54**(10), 1781–1785.
- Xu, J. and 10 others. 2010. A 108.83-m ice-core record of atmospheric dust deposition at Mt. Qomolangma (Everest), Central Himalaya. *Quat. Res.*, **73**(1), 33–38.
- Yao, T. and 7 others. 2002. Temperature and methane changes over the past 1000 years recorded in Dasuopu glacier (central Himalaya) ice core. *Ann. Glaciol.*, **35**, 379–383.

MS received 26 July 2010 and accepted in revised form 6 February 2011